

# Medium size macrocycles incorporating combinations of coordinated-1,3-diyne units, oxygen donors and group 14 elements

Robert C.J. Atkinson<sup>a</sup>, Louisa J. Hope-Weeks<sup>b,\*</sup>, Martin J. Mays<sup>a</sup>, Gregory A. Solan<sup>c,\*</sup>

<sup>a</sup> Department of Chemistry, Lensfield Road, Cambridge CB2 1EW, UK

<sup>b</sup> Department of Chemistry and Biochemistry, Texas Tech University, Lubbock, TX 79409-1061, USA

<sup>c</sup> Department of Chemistry, University of Leicester, University Road, Leicester LE1 7RH, UK

Received 1 December 2006; received in revised form 18 January 2007; accepted 18 January 2007

Available online 25 January 2007

## Abstract

Two approaches have been employed to prepare medium size macrocycles incorporating combinations of coordinated-1,3-diyne units, oxygen donors and group 14 elements. In the first approach, the acid-catalysed reaction of  $[\{\text{Co}_2(\text{CO})_6(\mu\text{-}\eta^2\text{-HOCH}_2\text{C}\equiv\text{C-})\}_2]$  (**1a**) with either  $\text{C}_6\text{H}_5\text{OH}$ ,  $\text{C}_6\text{H}_4\text{-1,4-(OH)}_2$  or  $\text{C}_6\text{H}_4\text{-1,2-(OH)}_2$  was found to form in good to moderate yield the nine-membered  $[\{\text{Co}_2(\text{CO})_6\}_2\{\text{cyclo-}\mu\text{-}\eta^2\text{:}\mu\text{-}\eta^2\text{-CH}_2\text{C}_2\text{C}_2\text{CH}_2\text{OC}_6\text{H}_4\}_2]$  (**2**) and the eight-membered macrocycles,  $[\{\text{Co}_2(\text{CO})_6\}_2\{\text{cyclo-}\mu\text{-}\eta^2\text{:}\mu\text{-}\eta^2\text{-CH}_2\text{C}_2\text{C}_2\text{CH}_2\text{-2,3-C}_6\text{H}_2\text{-1,4-(OH)}_2\}_2]$  (**3**) and  $[\{\text{Co}_2(\text{CO})_6\}_2\{\text{cyclo-}\mu\text{-}\eta^2\text{:}\mu\text{-}\eta^2\text{-CH}_2\text{C}_2\text{C}_2\text{CH}_2\text{-3,4-C}_6\text{H}_2\text{-1,2-(OH)}_2\}_2]$  (**4**), respectively. In contrast, treatment of the bis-lithiated derivative of **1a** with  $\text{Cl}_2\text{SiR}^1\text{R}^2$  affords the silicon-containing nine-membered macrocycles  $[\{\text{Co}_2(\text{CO})_6\}_2\{\text{cyclo-}\mu\text{-}\eta^2\text{:}\mu\text{-}\eta^2\text{-OCH}_2\text{C}_2\text{C}_2\text{CH}_2\text{OSiR}^1\text{R}^2\}_2]$  (**5a**  $\text{R}^1 = \text{R}^2 = \text{Me}$ ; **5b**  $\text{R}^1 = \text{R}^2 = \text{Ph}$ ; **5c**  $\text{R}^1 = \text{Me}$ ,  $\text{R}^2 = \text{Ph}$ ). Similarly, the germanium analogue of **5b**,  $[\{\text{Co}_2(\text{CO})_6\}_2\{\text{cyclo-}\mu\text{-}\eta^2\text{:}\mu\text{-}\eta^2\text{-OCH}_2\text{C}_2\text{C}_2\text{CH}_2\text{OGePh}_2\}_2]$  (**6**) can be prepared from  $\text{Cl}_2\text{GePh}_2$ . Single crystal X-ray diffraction studies have been reported on **2**, **3**, **5a**, **5b** and **6**.

© 2007 Elsevier B.V. All rights reserved.

**Keywords:** Macrocycle; Cobalt; Coordinated 1,3-diyne; Oxygen donor; Group 14

## 1. Introduction

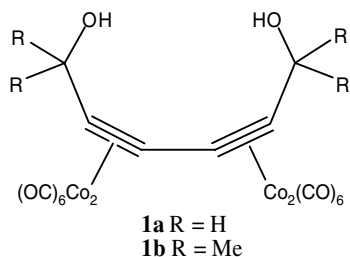
Despite the wide variety of synthetic organic strategies available to obtain five- and six-membered ring systems (e.g., via cyclisation and cycloaddition reactions), effective cyclisation routes to generate seven- to nine-membered rings remain relatively scarce [1]. This dearth in methodology can, in part, be attributed to entropic factors and transannular interactions that can often inhibit the reaction pathways for their synthesis [2]. To circumvent these difficulties in medium ring size synthesis, the use of metal-mediated approaches have started to come to the fore [1,3]. One such approach that has received some attention involves the use of dicobalt hexacarbonyl protected alkynyl groups

[4–6]. For example, medium (and large) size macrocycles containing a broad range of heteroatoms can be accessed by the use of  $\text{Co}_2(\text{CO})_6$ -coordinated 2-butyne-1,4-diols under Nicholas-type acid-catalysed reactions [5] or by employing salt elimination-type approaches [6].

Recently, we have been interested in incorporating 1,3-diyne fragments into macrocycles and have found that the acid-catalysed reaction of bis( $\text{Co}_2(\text{CO})_6$ )-coordinated diyne-diols, such as  $[\{\text{Co}_2(\text{CO})_6(\mu\text{-}\eta^2\text{-HOCH}_2\text{C}\equiv\text{C-})\}_2]$  (**1a**) (Fig. 1), with dithiol-based nucleophiles allows access to cyclothioalkynes with ring sizes of between 10 and 28 atoms [7]. Interestingly, the steric bulk of the coordinated diyne-diol employed has proved influential on product outcome with the seven-membered ring carbocycle  $[\{\text{Co}_2(\text{CO})_6\}_2\{\text{cyclo-}\mu\text{-}\eta^2\text{:}\mu\text{-}\eta^2\text{-C(=CH}_2\text{)CH}_2\text{CMe}_2\text{C}\equiv\text{C-C}\equiv\text{C}\}_2]$  being the only product formed when  $[\{\text{Co}_2(\text{CO})_6(\mu\text{-}\eta^2\text{-HOCHMe}_2\text{-C}\equiv\text{C-})\}_2]$  (**1b**) is employed as the starting material [8]. Indeed, the use of the potentially oxygen-centred nucleo-

\* Corresponding authors. Tel.: +44 (0)116 252 2096; fax: +44 (0)116 252 3789 (G.A. Solan).

E-mail address: gas8@leicester.ac.uk (G.A. Solan).

Fig. 1. Bis(Co<sub>2</sub>(CO)<sub>6</sub>)-coordinated diyne-diol **1a**.

philes, phenol or hydroquinone, in place of the thiol lead to the same strained carbocyclic product.

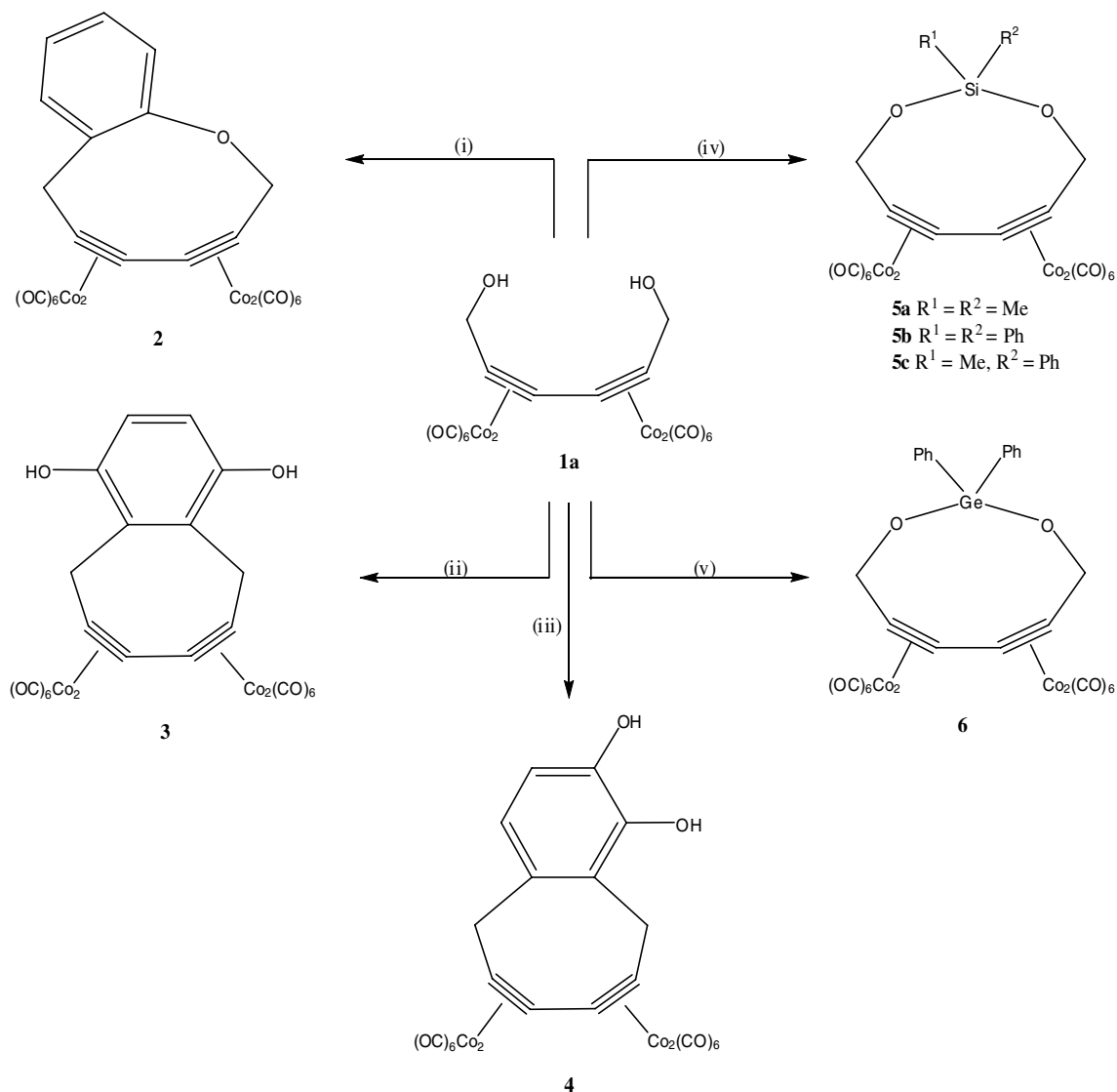
With the intent of forming medium ring size macrocycles incorporating 1,3-diyne, oxygen donors and group 14 elements, this article is concerned with investigating more thoroughly the reactivity of the less sterically encumbered **1a**. In the first instance, acid-catalysed conditions are

employed to study the reactivity of **1a** towards the aryl alcohols, phenol, hydroquinone and pyrocatechol. Secondly, we examine the use of the bis-lithiated derivative of **1a** as a means of introducing silicon and germanium into the macrocycle.

## 2. Results and discussion

### 2.1. Reaction with aryl alcohols

Reaction of **1a** [9] with one equivalent of phenol in dichloromethane, in the presence of HBF<sub>4</sub> · OEt<sub>2</sub>, affords [ $\{\text{Co}_2(\text{CO})_6\}_2\{\mu\text{-}\eta^2\text{:}\mu\text{-}\eta^2\text{-CH}_2\text{C}_2\text{C}_2\text{CH}_2\text{OC}_6\text{H}_4\}_2$ ] (**2**) (Scheme 1) along with trace quantities of the previously reported self-dimerised species [ $\{\text{Co}_2(\text{CO})_6\}_2\{\mu\text{-}\eta^2\text{:}\mu\text{-}\eta^2\text{-CH}_2\text{C}_2\text{C}_2\text{CH}_2\text{O}\}_2$ ] [10]. Use of aryl diols, hydroquinone and pyrocatechol, in place of phenol furnishes [ $\{\text{Co}_2(\text{CO})_6\}_2\{\mu\text{-}\eta^2\text{:}\mu\text{-}\eta^2\text{-CH}_2\text{C}_2\text{C}_2\text{CH}_2\text{-2,3-C}_6\text{H}_2\text{-1,4-(OH)}_2\}_2$ ] (**3**)



Scheme 1. Reagents and conditions: (i) C<sub>6</sub>H<sub>5</sub>OH, HBF<sub>4</sub> · OEt<sub>2</sub> (cat.), -78 °C, CH<sub>2</sub>Cl<sub>2</sub>; (ii) C<sub>6</sub>H<sub>4</sub>-1,4-(OH)<sub>2</sub>, HBF<sub>4</sub> · OEt<sub>2</sub> (cat.), -78 °C, CH<sub>2</sub>Cl<sub>2</sub>; (iii) C<sub>6</sub>H<sub>4</sub>-1,2-(OH)<sub>2</sub>, HBF<sub>4</sub> · OEt<sub>2</sub> (cat.), -78 °C, CH<sub>2</sub>Cl<sub>2</sub>; (iv) Cl<sub>2</sub>SiR<sup>1</sup>R<sup>2</sup>, 2 *n*-BuLi, -78 °C, THF; (v) Cl<sub>2</sub>GePh<sub>2</sub>, 2 *n*-BuLi, -78 °C, THF.

and  $[\{\text{Co}_2(\text{CO})_6\}_2 \{\text{cyclo-}\mu\text{-}\eta^2\text{:}\mu\text{-}\eta^2\text{-CH}_2\text{C}_2\text{C}_2\text{CH}_2\text{-3,4-C}_6\text{H}_2\text{-1,2-(OH)}_2\}]$  (**4**) as the only isolable products, respectively. Complexes **2–4** have been characterised by IR,  $^1\text{H}$  and  $^{13}\text{C}$  NMR spectroscopy and FAB mass spectrometry (Table 1 and Section 4). In addition, **2** and **3** have been the subject of single crystal X-ray diffraction studies.

Single crystals of **2** and **3** suitable for the X-ray determinations were both grown from dichloromethane solutions by slow diffusion of hexane at  $0^\circ\text{C}$ . Perspective views of **2** and **3** are depicted in Figs. 2 and 3; selected bond distances and angles are listed in Tables 2 and 3, respectively.

The molecular structure of **2** reveals the presence of a nine-membered  $\text{—C}\equiv\text{C—C}\equiv\text{C—C—C=C—O—C—}$  ring in which both alkyne units of the diyne are bound to  $\text{Co}_2(\text{CO})_6$  groups in an  $\eta^2\text{:}\eta^2$  fashion. The  $\text{Co}_2\text{C}_2$  cores adopt geometries approximating to tetrahedral with the bond parameters falling within the normal range [11,12]. The two  $\text{Co}_2\text{C}_2$  cores are arranged in a pseudo *cis* configuration [tors.: C(14)–C(15)–C(16)–C(17)  $33.1^\circ$ ] in a fashion similar to that in **1a** [9c], but unlike the *trans* configuration observed generally for other 1,3-diyne-tetracobalt compounds [12]. The two  $\text{C}_2\text{Co}_2(\text{CO})_6$  units are linked via a short C(15)–C(16) single bond 1.423(3) Å with the alkyne C–C bonds shorter [C(16)–C(17) 1.355(3), C(14)–C(15) 1.353(3) Å]. Some strain is apparent within the macrocycle with one of the alkyne *bend-back* angles [C(18)–C(17)–C(16)  $133.8(2)^\circ$  vs. C(13)–C(14)–C(15)  $140.8(2)^\circ$ ] being significantly lower than in related acyclic cobalt–alkyne complexes; the mean C–C≡C angle is  $141.31^\circ$  [13].

In contrast, the structure of **3** reveals the presence of a smaller ring in this case consisting of an eight-membered  $\text{—C}\equiv\text{C—C}\equiv\text{C—C—C=C—C—}$  carbocycle. The coordinated alkyne units of the 1,3-diyne moiety bridge the  $\text{Co}_2(\text{CO})_6$  groups with the  $\text{Co}_2\text{C}_2$  cores again adopting the expected pseudo tetrahedral geometries [11,12]. The reduction in ring size from nine to eight results in the relative configuration of the  $\text{Co}_2\text{C}_2$  units adopting a more regular *cis* configuration [tors.: C(2)–C(3)–C(4)–C(5)  $4.0^\circ$ ] and indeed in a manner similar to that observed in the seven-membered carbocycle  $[\{\text{Co}_2(\text{CO})_6\}_2 \{\text{cyclo-}\mu\text{-}\eta^2\text{:}\mu\text{-}\eta^2\text{-C(=CH}_2\text{)CH}_2\text{CMe}_2\text{C}\equiv\text{C—C}\equiv\text{C}\}]$  [8]. The alkyne *bend-back* angles [C(6)–C(5)–C(4)  $134.4(2)^\circ$  vs. C(1)–C(2)–C(3)  $133.5(2)^\circ$ ] are alike in size with the average value lower than that in **2** but slightly larger than in  $[\{\text{Co}_2(\text{CO})_6\}_2 \{\text{cyclo-}\mu\text{-}\eta^2\text{:}\mu\text{-}\eta^2\text{-C(=CH}_2\text{)CH}_2\text{CMe}_2\text{C}\equiv\text{C—C}\equiv\text{C}\}]$  [8].

The solution state properties of **2** and **3** are in accord with the solid state structures being maintained in solution (see Table 1). In the  $^1\text{H}$  NMR spectrum of **2**, two resonances are seen for the inequivalent methylene groups ( $\delta$  5.52, 4.18) whereas only one  $\text{CH}_2$  signal ( $\delta$  4.26) is seen for the more symmetrical **3**. The  $^{13}\text{C}$  NMR spectrum of **2** supports the inequivalency, with the  $\text{CH}_2$  carbons appearing at  $\delta$  69.9 and  $\delta$  39.2, the more downfield signal corresponding to the group adjacent to the oxygen atom. In **4**, the  $\text{CH}_2$  carbons appear as separate singlets ( $\delta$  30.0 and 29.7) in the  $^{13}\text{C}$  NMR spectrum while a broad resonance

Table 1  
Spectroscopic and analytical data for the new complexes **2–6**

Complex	$\nu(\text{CO})$ ( $\text{cm}^{-1}$ ) <sup>a</sup>	$^1\text{H}$ NMR ( $\delta$ ) <sup>b</sup>	FAB mass spectrum	Microanalysis (%) <sup>c</sup>	
				C	H
<b>2</b>	2031(s), 2056(s), 2084(s), 2100(m)	7.03–6.99(m, 4H, Ph), 5.52(s, 2H, CCH <sub>2</sub> O), 4.18(s, 2H, CCH <sub>2</sub> C)	$M^+$ (740), $M^+ - n\text{CO}$ ( $n = 4-12$ )	38.65 (38.95)	1.21 (1.09)
<b>3</b>	2030(s), 2042(s), 2063(vs), 2084(s), 2103(m)	6.98(s, 2H, OH), 6.80(s, 2H, Ph), 4.26(s, 4H, CCH <sub>2</sub> C)	$M^+$ (756), $M^+ - n\text{CO}$ ( $n = 2-8$ )	40.89 (40.58) <sup>d</sup>	1.99 (1.89) <sup>d</sup>
<b>4</b>	2023(s), 2037(s), 2061(vs), 2080(s), 2100(w)	7.05–6.40(m, 2H, Ph), 4.30(br s, 4H, CCH <sub>2</sub> C)	$M^+$ (756), $M^+ - n\text{CO}$ ( $n = 1-6$ )	–	–
<b>5a</b>	2026(s), 2062(vs), 2082(s), 2102(m)	5.07(s, 4H, CH <sub>2</sub> ), 0.22(s, 6H, Me)	$M^+$ (738), $M^+ - n\text{CO}$ ( $n = 1-12$ )	34.98 (35.35) <sup>d</sup>	2.02 (2.17) <sup>d</sup>
<b>5b</b>	2026(s), 2063(vs), 2083(m), 2103(m)	7.77–7.29(m, 10H, Ph), 5.04(s, 4H, CH <sub>2</sub> )	$M^+$ (862), $M^+ - n\text{CO}$ ( $n = 5-12$ )	44.01 (43.78) <sup>d</sup>	2.09 (2.34) <sup>d</sup>
<b>5c</b>	2029(s), 2061(vs), 2083(s), 2103(m)	7.70–7.38(m, 5H, Ph), 5.00(s, 4H, CH <sub>2</sub> ), 0.40(s, 3H, Me)	$M^+$ (800), $M^+ - n\text{CO}$ ( $n = 1-12$ )	37.53 (37.51)	1.61 (1.50)
<b>6</b>	2072(s), 2060(vs), 2084(s), 2102(m)	7.74–7.44(m, 10H, Ph), 5.05(s, 4H, CH <sub>2</sub> )	$M^+$ (907), $M^+ - n\text{CO}$ ( $n = 1-12$ )	39.44 (39.72)	1.48 (1.55)

<sup>a</sup> Recorded in  $\text{CH}_2\text{Cl}_2$  in 0.5 mm NaCl solution cells.

<sup>b</sup>  $^1\text{H}$  NMR chemical shifts in ppm relative to  $\text{SiMe}_4$  (0.0 ppm), coupling constants in Hz in  $\text{CDCl}_3$  at 293 K.

<sup>c</sup> Calculated values shown in parentheses.

<sup>d</sup> Calculated values include 0.5 hexane.

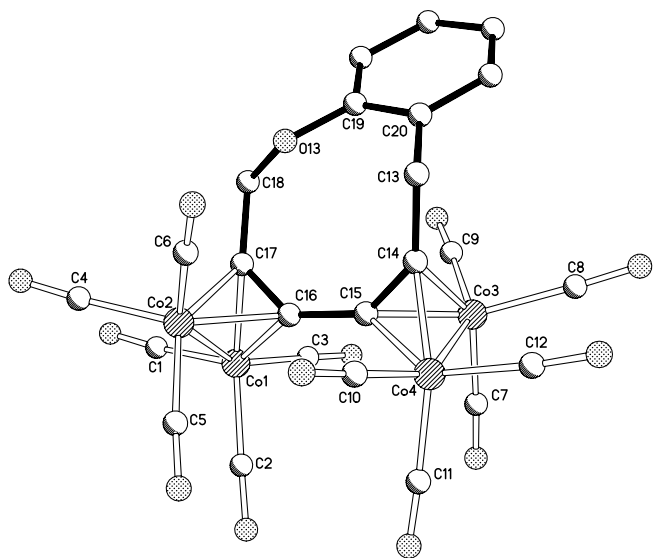


Fig. 2. Molecular structure of **2** with partial atom labeling scheme; all hydrogen atoms have been omitted for clarity.

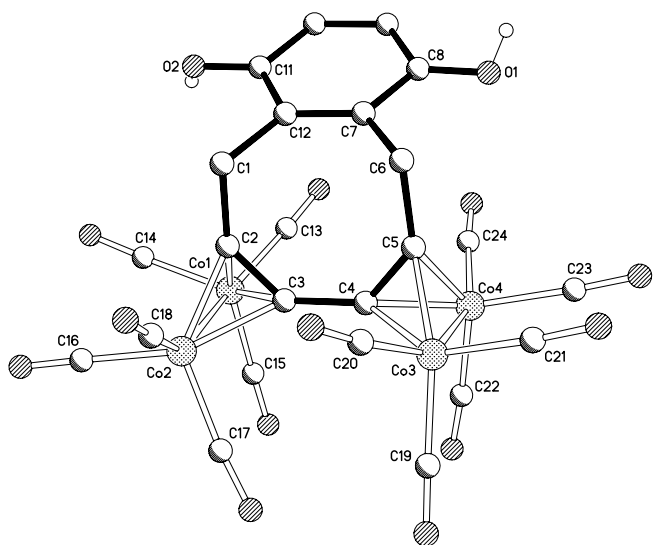


Fig. 3. Molecular structure of **3** with partial atom labeling scheme; all hydrogen atoms have been omitted for clarity.

at  $\delta$  4.30 is seen for the  $\text{CH}_2$  protons in the  $^1\text{H}$  NMR spectrum. The IR spectra for **2–4** reveal terminal carbonyl bands with a pattern similar to that in **1a** [9] as well as to those of other bis(dicobalt hexacarbonyl)-protected 1,3-diyne complexes [12]. In the FAB mass spectra molecular ions are seen for all three complexes along with fragmentation peaks corresponding to the loss of carbonyl groups from the molecular ions.

The proposed pathway by which **2–4** are formed is shown in Scheme 2. The initial step for all three products is the formation of the propargylium carbocation intermediate **A** on reaction with  $\text{HBF}_4$  [14]. The relatively unhindered **A** (cf. the carbocation of **1b**) can then undergo electrophilic attack at the most electron rich sites on the

Table 2  
Selected bond distances ( $\text{\AA}$ ) and angles ( $^\circ$ ) for **2**

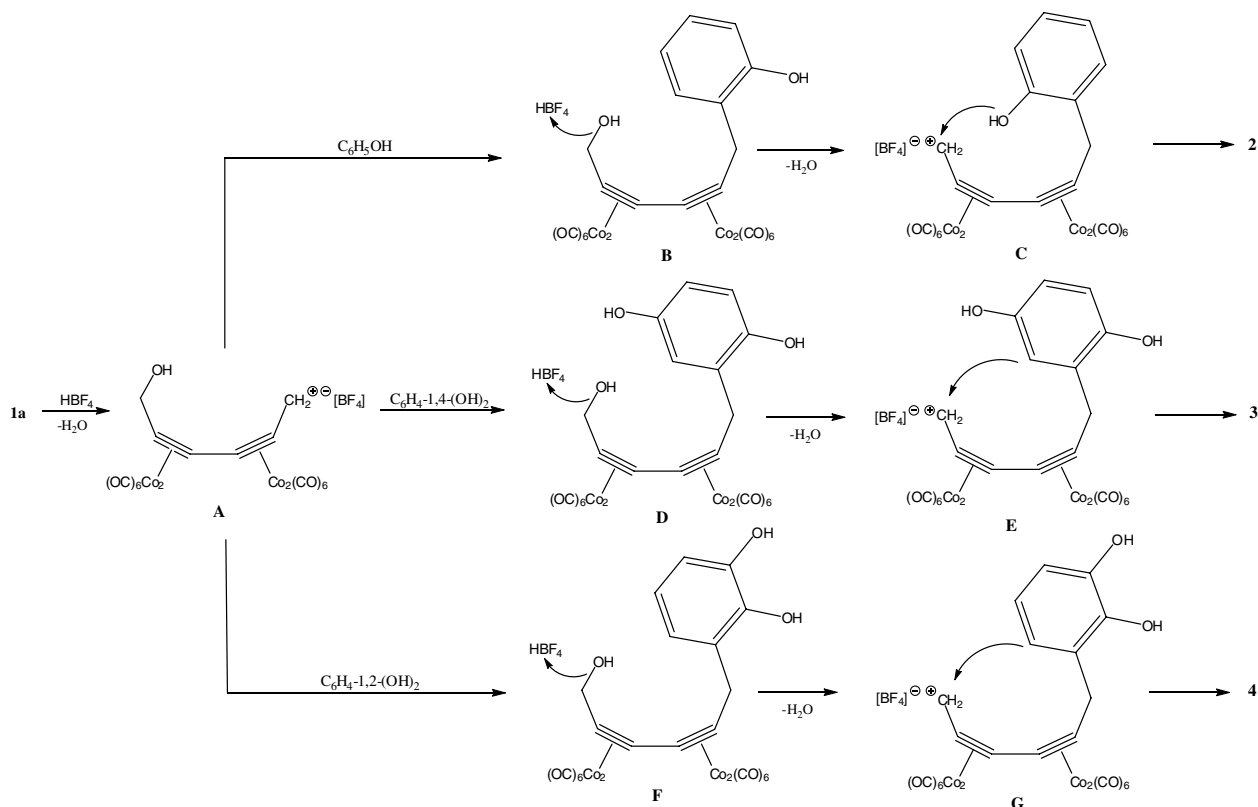
Bond lengths			
Co(1)–C(17)	1.946(2)	O(13)–C(18)	1.446(2)
Co(1)–C(16)	1.966(2)	C(13)–C(14)	1.503(3)
Co(1)–Co(2)	2.4795(4)	C(13)–C(20)	1.515(3)
Co(2)–C(17)	1.957(2)	C(14)–C(15)	1.353(3)
Co(2)–C(16)	1.966(2)	C(15)–C(16)	1.423(3)
Co(3)–C(14)	1.958(2)	C(16)–C(17)	1.355(3)
Co(3)–C(15)	1.969(2)	C(17)–C(18)	1.486(3)
Co(3)–Co(4)	2.4744(4)	C(19)–C(20)	1.387(3)
Co(4)–C(14)	1.954(2)	Co–C(carbonyl)	1.791(2)–1.828(3)
Co(4)–C(15)	1.960(2)	C–O(carbonyl)	1.125(4)–1.139(4)
O(13)–C(19)	1.382(3)		
Bond angles			
C(17)–Co(1)–C(16)	40.52(8)	C(15)–Co(4)–Co(3)	51.13(6)
C(17)–Co(1)–Co(2)	50.74(6)	C(19)–O(13)–C(18)	117.5(2)
C(16)–Co(1)–Co(2)	50.91(6)	C(14)–C(13)–C(20)	112.1(2)
C(17)–Co(2)–C(16)	40.41(8)	C(15)–C(14)–C(13)	140.8(2)
C(17)–Co(2)–Co(1)	50.38(6)	C(14)–C(15)–C(16)	139.0(2)
C(16)–Co(2)–Co(1)	50.90(6)	C(17)–C(16)–C(15)	137.3(2)
C(14)–Co(3)–C(15)	40.30(8)	C(16)–C(17)–C(18)	133.8(2)
C(14)–Co(3)–Co(4)	50.69(6)	O(13)–C(18)–C(17)	106.2(2)
C(15)–Co(3)–Co(4)	50.81(6)	O(13)–C(19)–C(20)	116.9(2)
C(14)–Co(4)–C(15)	40.44(8)	C(19)–C(20)–C(13)	121.4(2)
C(14)–Co(4)–Co(3)	50.83(6)		

aryl alcohols which will be the carbon atoms *ortho* to a hydroxyl group to give **B**, **D** and **F** [15]. Carbocations **C**, **E** and **G** can then be generated by removal of  $\text{OH}^-$  from **B**, **D** and **F** on reaction with  $\text{H}^+$ , respectively. A second electrophilic attack can occur in each pathway at the most accessible and nucleophilic site on the linked aryl alcohol to afford **2**, **3** and **4**.

It might be argued that the 4 position in the phenol moiety in **C** is the most activated position for electrophilic attack [15] but it is likely that the ensuing strain that would occur in the

Table 3  
Selected bond distances ( $\text{\AA}$ ) and angles ( $^\circ$ ) for **3**

Bond lengths			
Co(1)–C(2)	1.953(3)	C(3)–C(4)	1.449(4)
Co(1)–C(3)	1.974(3)	C(5)–C(6)	1.500(4)
Co(1)–Co(2)	2.4629(5)	C(6)–C(7)	1.499(4)
Co(2)–C(2)	1.961(3)	C(7)–C(8)	1.489(4)
Co(2)–C(3)	1.969(3)	C(8)–C(9)	1.464(4)
Co(3)–C(5)	1.955(3)	C(9)–C(10)	1.327(4)
Co(3)–C(4)	1.974(3)	C(11)–C(12)	1.482(4)
Co(4)–C(5)	1.959(3)	C(12)–C(1)	1.508(4)
Co(4)–C(4)	1.962(3)	Co–C(carbonyl)	1.789(3)–1.830(3)
C(1)–C(2)	1.505(4)	C–O(carbonyl)	1.125(4)–1.139(4)
C(2)–C(3)	1.342(4)		
Bond angles			
C(2)–Co(1)–C(3)	39.97(10)	C(5)–Co(4)–Co(3)	51.04(8)
C(2)–Co(1)–Co(2)	51.15(7)	C(4)–Co(4)–Co(3)	51.58(8)
C(3)–Co(1)–Co(2)	51.26(7)	C(2)–C(1)–C(12)	109.3(2)
C(2)–Co(2)–C(3)	39.94(10)	C(3)–C(2)–C(1)	133.5(2)
C(2)–Co(2)–Co(1)	50.87(8)	C(2)–C(3)–C(4)	132.7(2)
C(3)–Co(2)–Co(1)	51.44(8)	C(5)–C(4)–C(3)	131.8(2)
C(5)–Co(3)–C(4)	40.18(11)	C(4)–C(5)–C(6)	134.4(2)
C(5)–Co(3)–Co(4)	51.18(8)	C(7)–C(6)–C(5)	112.1(2)
C(4)–Co(3)–Co(4)	51.14(8)	C(8)–C(7)–C(6)	115.9(2)
C(5)–Co(4)–C(4)	40.27(11)	C(7)–C(12)–C(1)	124.3(3)

Scheme 2. Proposed pathway for the formation of **2**, **3** and **4**.

resulting product drives the attack to occur at the next most active site, the oxygen atom. In the case of **E** and **G**, both steric and electronic factors favour the reaction taking place at the 3 (**E**) or 4 positions (**G**) on the ring. Interestingly, the related methylene-spaced diyne complex  $[\{\text{Co}_2(\text{CO})_6(\mu-\eta^2:\mu-\eta^2\text{-HOCH}_2\text{C}\equiv\text{C}-\text{CH}_2-\text{C}\equiv\text{C}-\text{CH}_2\text{OH})\}_2]$  does undergo 2,4 additions with  $\text{C}_6\text{H}_5\text{OMe}$  and  $1,3\text{-C}_6\text{H}_4(\text{OMe})_2$ ; the additional flexibility of this particular diyne may in part explain this difference in reactivity [16].

## 2.2. Reaction with chloro-silanes and -germanes

Treatment of an equimolar mixture of **1a** and  $\text{Cl}_2\text{SiR}^1\text{R}^2$  ( $\text{R}^1 = \text{R}^2 = \text{Me}$ , Ph or  $\text{R}^1 = \text{Me}$ ,  $\text{R}^2 = \text{Ph}$ ) with two equivalents of *n*-BuLi in THF at  $-78^\circ\text{C}$  gave in good yield  $[\{\text{Co}_2(\text{CO})_6\}_2\{\mu-\eta^2:\mu-\eta^2\text{-OCH}_2\text{C}_2\text{C}_2\text{CH}_2\text{OSiR}^1\text{R}^2\}]$  (**5a**  $\text{R}^1 = \text{R}^2 = \text{Me}$ ; **5b**  $\text{R}^1 = \text{R}^2 = \text{Ph}$ ; **5c**  $\text{R}^1 = \text{Me}$ ,  $\text{R}^2 = \text{Ph}$ ) (Scheme 1). Complexes **5a–5c** have been characterised by FAB mass spectrometry and by IR,  $^1\text{H}$  and  $^{13}\text{C}$  NMR spectroscopy (see Table 1 and Section 4). Satisfactory microanalyses were obtained for all complexes. Additionally, complexes **5a** and **5b** have been the subject of single crystal X-ray diffraction studies.

Suitable crystals of **5a** and **5b** were grown from dichloromethane solutions by slow diffusion of hexane at  $0^\circ\text{C}$ . The molecular structures are similar and will be discussed together. A view of **5a** is depicted in Fig. 4; selected bond distances and angles for both structures are listed in Table 4. Both structures reveal the formation of symmetrical

nine-membered  $-\text{C}\equiv\text{C}-\text{C}\equiv\text{C}-\text{C}-\text{O}-\text{Si}-\text{O}-\text{C}-$  rings with **5a** containing two methyl substituents on silicon and **5b** two phenyl groups. The dicobalt bound alkyne units adopt the usual pseudo tetrahedral geometries with all bond lengths falling in the normal ranges [11,12]. As with **2**, the two  $\text{Co}_2\text{C}$  units are disposed in a pseudo *cis* configuration [tors.:  $\text{C}(14)-\text{C}(15)-\text{C}(16)-\text{C}(17)$   $35.3^\circ$  (**5a**),  $34.1^\circ$  (**5b**)] while the larger *bend-back* angles [ $\text{C}(13)-\text{C}(14)-\text{C}(15)$   $138.2(2)^\circ$  (**5a**),  $138.0(3)^\circ$  (**5b**);  $\text{C}(18)-\text{C}(17)-\text{C}(16)$

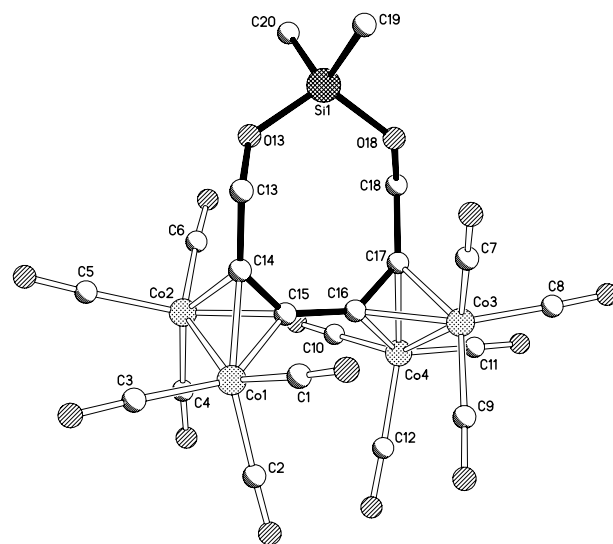
Fig. 4. Molecular structure of **5a** with partial atom labeling scheme; all hydrogen atoms have been omitted for clarity.



Table 4  
Selected bond distances (Å) and angles (°) for **5a** and **5b**

	<b>5a</b>	<b>5b</b>		<b>5a</b>	<b>5b</b>
<i>Bond lengths</i>					
Si(1)–O(13)	1.643(2)	1.635(2)	C(16)–C(17)	1.350(3)	1.356(5)
Si(1)–O(18)	1.644(2)	1.641(2)	C(17)–C(18)	1.494(3)	1.475(5)
Si(1)–C(20) <sub>methyl</sub>	1.844(2)	–	C(18)–O(18)	1.428(3)	1.427(4)
Si(1)–C(19) <sub>methyl</sub>	1.849(3)	–	Co(1)–Co(2)	2.4734(4)	2.4757(7)
Si(1)–C(19) <sub>phenyl</sub>	–	1.853(4)	Co(3)–Co(4)	2.4789(4)	2.4780(7)
Si(1)–C(25) <sub>phenyl</sub>	–	1.856(4)	C <sub>alkyne</sub> –Co(1)	1.950(2)–1.957(2)	1.933(4)–1.969(4)
C(13)–O(13)	1.423(3)	1.419(4)	C <sub>alkyne</sub> –Co(2)	1.947(2)–1.964(2)	1.960(3)–1.962(3)
C(13)–C(14)	1.487(3)	1.490(5)	C <sub>alkyne</sub> –Co(3)	1.953(2)–1.963(2)	1.964(3)–1.966(3)
C(14)–C(15)	1.350(3)	1.355(4)	C <sub>alkyne</sub> –Co(4)	1.940(2)–1.974(2)	1.942(4)–1.967(3)
C(15)–C(16)	1.427(3)	1.433(5)	Co–C(carbonyl)	1.787(3)–1.832(3)	1.799(5)–1.835(5)
			C–O(carbonyl)	1.127(3)–1.138(3)	1.125(4)–1.136(5)
<i>Bond angles</i>					
O(13)–Si(1)–O(18)	112.25(8)	114.31(13)	C(17)–Co(4)–Co(3)	50.69(6)	51.01(10)
C(14)–Co(1)–C(15)	40.44(9)	40.63(13)	C(16)–Co(4)–Co(3)	50.79(9)	50.93(9)
C(14)–Co(1)–Co(2)	50.57(6)	50.98(10)	C(13)–O(13)–Si(1)	128.40(14)	126.3(2)
C(15)–Co(1)–Co(2)	51.03(6)	50.85(10)	O(13)–C(13)–C(14)	110.2(2)	111.0(3)
C(14)–Co(2)–C(15)	40.38(9)	40.43(13)	C(18)–O(18)–Si(1)	128.37(15)	125.4(2)
C(14)–Co(2)–Co(1)	50.65(6)	50.02(10)	C(15)–C(14)–C(13)	138.2(2)	138.0(3)
C(15)–Co(2)–Co(1)	50.74(6)	51.09(10)	C(14)–C(15)–C(16)	140.0(2)	140.3(3)
C(17)–Co(3)–C(16)	40.32(9)	40.39(14)	C(17)–C(16)–C(15)	140.2(2)	138.8(3)
C(17)–Co(3)–Co(4)	50.22(6)	50.23(10)	C(16)–C(17)–C(18)	137.6(2)	139.1(3)
C(16)–Co(3)–Co(4)	51.18(6)	50.95(10)	O(18)–C(18)–C(17)	109.6(2)	110.1(3)
C(17)–Co(4)–C(16)	40.35(9)	40.60(14)			

137.6(2)° (**5a**); 139.1(3)° (**5b**)] indicate that the C–C≡C sections of the rings are less strained than in **2**. The variation in silicon substituents between **5a** and **5b** has some minor effects on the ring parameters which is mostly driven by the O(13)–Si(1)–O(18) angle for **5b** [114.31(13)°] being larger than for **5a** [112.25(8)°].

The <sup>1</sup>H NMR spectra of **5a–5c** are all very similar with the equivalent methylene protons being seen ca. δ 5.0; in the case of **5a** and **5c** additional signals for the Si–CH<sub>3</sub> protons are seen as singlets at ca. δ 0.3. In the IR spectra four absorption bands in the terminal carbonyl region are seen in a pattern similar to other complexes of this class [11,12]. As with **2–4**, complexes **5a–5c** gave molecular ions peaks in their FAB mass spectra along with peaks corresponding to the loss of carbonyl groups from the molecular ion.

To examine the effect of introducing a larger group 14 atom into the macrocycle we have prepared the germanium analogue of **5b**, [{Co<sub>2</sub>(CO)<sub>6</sub>}]<sub>2</sub>{μ-η<sup>2</sup>:μ-η<sup>2</sup>-OCH<sub>2</sub>C<sub>2</sub>C<sub>2</sub>-CH<sub>2</sub>OGePh<sub>2</sub>} (**6**) by reacting **1a** with Cl<sub>2</sub>GePh<sub>2</sub> and two equivalents of *n*-BuLi (Scheme 1). Following work up, complex **6** could be isolated in good yield and has been fully characterised by FAB mass spectrometry, <sup>1</sup>H, <sup>13</sup>C NMR and IR spectroscopy (see Table 1 and Section 4). The spectroscopic properties of **6** are similar to those of **5b** with four carbonyl absorption bands apparent in the IR spectrum and the methylene protons clearly visible as singlets at δ 5.05 in the <sup>1</sup>H NMR spectrum. In the mass spectrum a molecular ion peak is seen along with fragmentation peaks corresponding to loss of CO groups. Crystals of **6** suitable for a single crystal X-ray diffraction study could also be obtained from a dichloromethane solution by slow diffusion of hexane at 0 °C.

The molecular structure of **6** is shown in Fig. 5; selected bond distances and angles are collected in Table 5. The structure resembles **5b** with a nine-membered macrocycle bound at the alkyne moieties by two Co<sub>2</sub>(CO)<sub>6</sub> units but differs with a germanium atom in place of silicon within the ring. This variation has little effect on the *bend-back* angles [C(13)–C(14)–C(15) 138.2(2)° (**6**), 138.0(3)° (**5b**); C(18)–C(17)–C(16) 140.8(3)° (**6**), 139.1(3)° (**5b**)] but does influence the relative disposition of the two Co<sub>2</sub>C<sub>2</sub> units with a more regular *cis* configuration apparent in **6** [tors.: C(14)–C(15)–C(16)–C(18) 25.2° (**6**), 34.1° (**5b**)]. Some dif-

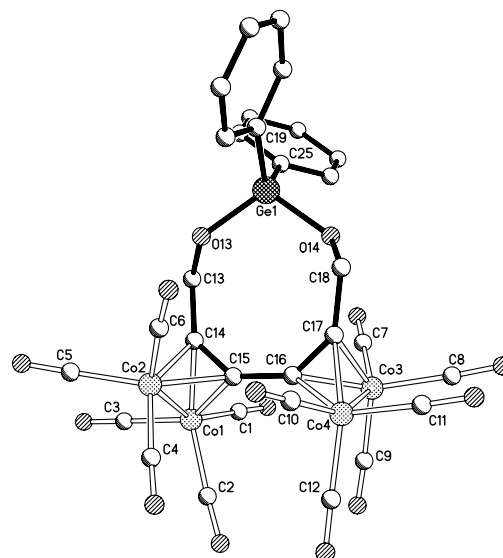


Fig. 5. Molecular structure of **6** with partial atom labeling scheme; all hydrogen atoms have been omitted for clarity.

Table 5  
Selected bond distances (Å) and angles (°) for **6**

Bond lengths			
Co(1)–C(14)	1.953(3)	Ge(1)–C(19)	1.932(3)
Co(1)–C(15)	1.969(3)	Ge(1)–C(25)	1.927(3)
Co(1)–Co(2)	2.4694(6)	C(13)–O(13)	1.436(3)
Co(2)–C(14)	1.956(3)	C(13)–C(14)	1.497(4)
Co(2)–C(15)	1.968(3)	C(14)–C(15)	1.351(4)
Co(3)–C(17)	1.960(3)	C(15)–C(16)	1.424(4)
Co(3)–C(16)	1.969(3)	C(16)–C(17)	1.352(4)
Co(3)–Co(4)	2.4719(6)	C(17)–C(18)	1.487(4)
Co(4)–C(17)	1.945(3)	C(18)–O(14)	1.430(3)
Co(4)–C(16)	1.980(3)	Co–C(carbonyl)	1.781(4)–1.833(4)
Ge(1)–O(13)	1.777(2)	C–O(carbonyl)	1.129(4)–1.135(4)
Ge(1)–O(14)	1.780(2)		
Bond angles			
O(13)–Ge(1)–O(14)	108.17(9)	C(17)–Co(4)–Co(3)	51.00(9)
C(14)–Co(1)–C(15)	40.31(11)	C(16)–Co(4)–Co(3)	51.04(9)
C(14)–Co(1)–Co(2)	50.86(9)	C(13)–O(13)–Ge(1)	119.9(2)
C(15)–Co(1)–Co(2)	51.12(9)	O(13)–C(13)–C(14)	110.0(2)
C(14)–Co(2)–C(15)	40.30(12)	C(18)–O(14)–Ge(1)	121.0(2)
C(14)–Co(2)–Co(1)	50.78(8)	C(15)–C(14)–C(13)	138.2(3)
C(15)–Co(2)–Co(1)	51.18(8)	C(14)–C(15)–C(16)	140.5(3)
C(17)–Co(3)–C(16)	40.24(12)	C(17)–C(16)–C(15)	140.2(3)
C(17)–Co(3)–Co(4)	50.45(8)	C(16)–C(17)–C(18)	140.8(3)
C(16)–Co(3)–Co(4)	51.44(8)	O(14)–C(18)–C(17)	109.4(2)
C(17)–Co(4)–C(16)	40.28(12)		

ferences are also evident within the C–O–E–O–C (E = Si, Ge) section of the macrocycle with a compression of all the O–E–O and E–O–C bond angles apparent in the germanium derivative **6** [O–E(1)–O 108.17(9)° (**6**) vs. 114.31(13)° (**5b**); E(1)–O–C 121.0(2), 119.9(2) (**6**) vs. 126.3(2), 125.4(2) (**5b**)].

### 3. Conclusions

In this study, we have shown that both an acid-catalysed condensation route and a metathesis-type approach can be successfully employed to prepare strained eight- (**3**, **4**) and nine-membered (**2**, **5a–c**, **6**) macrocycles containing combinations of coordinated 1,3-diyne units, oxygen donors and group 14 elements. Unlike the more sterically bulky **1b**, **1a** undergoes Nicholas-type reactions with hydroxyl arenes to afford products that are the result of functionalisation at both O and C sites within the arene (**2–4**). Incorporation of silicon or germanium into the macrocycle (**5a–5c**, **6**) has demonstrated that the size of the group 14 element can influence structural features within the macrocycle.

### 4. Experimental

#### 4.1. General procedures and materials

Unless otherwise stated all experiments were carried out under an atmosphere of dry, oxygen-free nitrogen, using standard Schlenk line techniques and solvents freshly distilled from appropriate drying agent [17]. Except where otherwise indicated NMR spectra were recorded in CDCl<sub>3</sub> using a Bruker DRX 400 spectrometer with TMS as an

external standard for <sup>1</sup>H and <sup>13</sup>C spectra. Infrared spectra were, unless otherwise stated, recorded in dichloromethane solution in 0.5 mm NaCl solution cells, using a Perkin–Elmer 1710 Fourier Transform Spectrometer. FAB (Fast atom bombardment) mass spectra were recorded using a Kratos MS 890 instrument with 3-nitrobenzyl alcohol as matrix. Elemental analyses were performed at the University of Cambridge. Preparative TLC was carried out on 1 mm silica plates prepared at the University of Cambridge. Column chromatography was performed on Kieselgel 60 (70–230 mesh ASTM). All products are listed in order of decreasing R<sub>f</sub>. The reagents, phenol, hydroquinone, pyrocatechol, tetrafluoroboric acid (54 wt. % in diethylether), *n*-butyllithium (1.6 M in hexane), dichlorodimethylsilane, dichlorodiphenylsilane, dichloro(methyl)phenylsilane and diphenylgermanium dichloride were obtained from Aldrich Chemical Co. and used without further purification. [ $\{Co_2(CO)_6(\mu-\eta^2-HOCH_2C\equiv C-)\}_2$ ] (**1a**) was prepared by the literature method [9].

#### 4.2. Synthesis of [ $\{Co_2(CO)_6\}_2\{\mu-\eta^2:\mu-\eta^2-CH_2C_2C_2CH_2OC_6H_4\}$ ] (**2**)

To a stirred solution of **1a** (0.50 g, 0.733 mmol) and C<sub>6</sub>H<sub>5</sub>OH (0.07 mL, 0.797 mmol) in dichloromethane (150 mL) at –78 °C was added six drops of HBF<sub>4</sub>·OEt<sub>2</sub>. The solution was warmed to 30 °C and after 4 h an excess of sodium hydrogen carbonate was added. The solvent was removed on the rotary evaporator, the residue dissolved in hexane and the solution filtered through a plug of magnesium sulfate. The solution was adsorbed onto silica, the silica pumped dry and added to the top of a chromatography column. Elution with hexane:dichloromethane (8:1) afforded orange crystalline [ $\{Co_2(CO)_6\}_2\{\mu-\eta^2:\mu-\eta^2-CH_2C_2C_2CH_2O\}_2$ ] (0.04 g, 4%) [10]. Further elution of the column with hexane:dichloromethane (7:1) afforded deep red crystalline **2** (0.51 g, 94%). <sup>13</sup>C {<sup>1</sup>H} NMR (CDCl<sub>3</sub>): δ 199.6 (CO), 136.2–124.3 (Ph), 96.2, 82.4 (C≡C), 69.9 (OCH<sub>2</sub>), 39.2 (CCH<sub>2</sub>).

#### 4.3. Synthesis of [ $\{Co_2(CO)_6\}_2\{\mu-\eta^2:\mu-\eta^2-CH_2C_2C_2CH_2-2,3-C_6H_2-1,4-(OH)_2\}$ ] (**3**)

To a stirred solution of **1a** (0.50 g, 0.733 mmol) and C<sub>6</sub>H<sub>4</sub>-1,4-(OH)<sub>2</sub> (0.081 g, 0.736 mmol) in dichloromethane (150 mL) at –78 °C was added 10 drops of HBF<sub>4</sub>·OEt<sub>2</sub>. The solution was warmed to 30 °C and after 4 h an excess of sodium hydrogen carbonate was added. The solvent was removed on the rotary evaporator, the residue dissolved in hexane and the solution filtered through a plug of magnesium sulfate. The solution was adsorbed onto silica, the silica pumped dry and added to the top of a chromatography column. Elution with hexane:dichloromethane (2:1) afforded green crystalline **3** (0.14 g, 25%) along with several minor unidentified products. <sup>13</sup>C {<sup>1</sup>H} NMR (CDCl<sub>3</sub>): δ 198.6 (CO), 136.3 (Ph), 98.6, 92.2 (C≡C), 31.3 (CH<sub>2</sub>).

#### 4.4. Synthesis of [ $\{Co_2(CO)_6\}_2\{cyclo-\mu-\eta^2-\mu-\eta^2-CH_2C_2C_2CH_2-3,4-C_6H_2-1,2-(OH)_2\}$ ] (**4**)

To a stirred solution of **1a** (0.250 g, 0.367 mmol) and  $C_6H_4-1,2-(OH)_2$  (0.040 g, 0.367 mmol) in dichloromethane (70 mL) at  $-78^\circ C$  was added five drops of  $HBF_4 \cdot OEt_2$ . The solution was warmed to room temperature and after 3 h an excess of sodium hydrogen carbonate was added. The solvent was removed on the rotary evaporator, the residue dissolved in hexane and the solution filtered through a plug of magnesium sulfate. The filtrate was concentrated and dissolved in the minimum quantity of dichloromethane and applied to the base of TLC plates. Elution with hexane:ethyl acetate (3:1) afforded trace quantities of a green solid which decomposed in air and green crystalline **4** (0.11 g, 40%).  $^{13}C \{^1H\}$  NMR ( $CDCl_3$ ):  $\delta$  199.0 (CO), 143.4, 133.9, 126.9 (Ph, C), 121.8, 113.6 (Ph, CH), 97.4, 93.9 ( $C\equiv C$ ), 30.0, 29.7 ( $CH_2$ ).

#### 4.5. Synthesis of [ $\{Co_2(CO)_6\}_2\{\mu-\eta^2-\mu-\eta^2-OCH_2C_2C_2CH_2OSiR^1R^2\}$ ] (**5**)

##### 4.5.1. $R^1 = R^2 = Me$ (**5a**)

To a solution of **1a** (1.00 g, 1.466 mmol) and  $Cl_2SiMe_2$  (0.20 mL, 1.650 mmol) in tetrahydrofuran (150 mL) at

$-78^\circ C$ , was added *n*-BuLi (1.84 mL, 2.932 mmol). The solution was allowed to warm to room temperature and after 3 h the mixture was filtered through a florasil pad ( $2 \times 5$  cm). The solvent was removed on a rotary evaporator, the residue dissolved in dichloromethane and adsorbed onto florasil. The florasil was pumped dry and added to the top of a chromatography column. Elution with hexane afforded red crystalline **5a** (0.74 g, 68%).  $^{13}C \{^1H\}$  NMR ( $CDCl_3$ ):  $\delta$  199.0 (CO), 99.9, 96.8 ( $C\equiv C$ ), 65.9 ( $CH_2$ ),  $-3.7$  (Me).

##### 4.5.2. $R^1 = R^2 = Ph$ (**5b**)

Complex **1a** (1.00 g, 1.466 mmol) and  $Cl_2SiPh_2$  (0.31 mL, 1.470 mmol) were used in a procedure analogous to that outlined for **5a** above. Elution with hexane afforded deep red crystalline **5b** (0.68 g, 54%).  $^{13}C \{^1H\}$  NMR ( $CDCl_3$ ):  $\delta$  199.4 (CO), 134.9, 127.9 (Ph), 98.6, 94.2 ( $C\equiv C$ ), 63.8 ( $CH_2$ ).

##### 4.5.3. $R^1 = Me, R^2 = Ph$ (**5c**)

Complex **1a** (0.50 g, 0.733 mmol) and  $Cl_2SiPh_2$  (0.12 mL, 0.738 mmol) were used in a procedure analogous to that outlined for **5a** above. Elution with hexane afforded deep red crystalline **5c** (0.43 g, 73%).  $^{13}C \{^1H\}$  NMR ( $CDCl_3$ ):  $\delta$  199.1 (CO), 138.2, 134.6, 128.0 (Ph), 99.8, 93.4 ( $C\equiv C$ ), 63.7 ( $CH_2$ ),  $-3.9$  (Me).

Table 6  
Crystallographic and data processing parameters for **2**, **3**, **5a**, **5b** and **6**

Complex	<b>2</b>	<b>3</b>	<b>5a</b>	<b>5b</b>	<b>6</b>
Formula	$C_{24}H_8Co_4O_{13}$	$C_{24}H_8Co_4O_{14}$	$C_{20}H_{10}Co_4SiO_{14}$	$C_{30}H_{14}Co_4SiO_{14}$	$C_{30}H_{14}Co_4GeO_{14}$
<i>M</i>	740.02	756.02	738.09	862.22	906.72
Crystal size (mm <sup>3</sup> )	$0.21 \times 0.16 \times 0.09$	$0.14 \times 0.09 \times 0.07$	$0.23 \times 0.18 \times 0.14$	$0.18 \times 0.18 \times 0.10$	$0.16 \times 0.09 \times 0.07$
Temperature (K)	180(2)	180(2)	180(2)	180(2)	180(2)
Crystal system	Monoclinic	Monoclinic	Monoclinic	Monoclinic	Triclinic
Space group	$P2_1/c$	$P2_1/n$	$P2_1/c$	$C2/c$	$P\bar{1}$
<i>a</i> (Å)	9.3263(3)	8.7296(6)	11.2461(4)	15.7670(6)	10.3893(4)
<i>b</i> (Å)	17.5768(4)	26.5809(15)	15.2267(3)	10.3300(3)	12.6771(4)
<i>c</i> (Å)	16.6240(5)	11.9085(9)	15.8828(6)	41.4990(14)	13.9232(5)
$\alpha$ (°)	90	90	90	90	97.582(2)
$\beta$ (°)	99.287(2)	101.822(3)	98.743(2)	100.5810(15)	110.257(2)
$\gamma$ (°)	90	90	90	90	96.842(2)
<i>U</i> (Å <sup>3</sup> )	2689.39(13)	2704.6(3)	2688.18(15)	6644.1(4)	1678.31(10)
<i>Z</i>	4	4	4	8	2
<i>D<sub>c</sub></i> (Mg m <sup>-3</sup> )	1.828	1.857	1.824	1.724	1.794
<i>F</i> (000)	1456	1488	1456	3424	892
$\mu$ (Mo K $\alpha$ ) (mm <sup>-1</sup> )	2.490	2.481	2.536	2.066	2.887
Reflections collected	16449	26677	10610	8560	20815
Independent reflections	6086	4713	6163	5797	7601
<i>R<sub>int</sub></i>	0.0449	0.0628	0.0288	0.0290	0.0768
Restraints/parameters	0/370	209/379	0/354	0/442	0/442
Final <i>R</i> indices ( $I > 2\sigma(I)$ )	$R_1 = 0.0313$ $wR_2 = 0.0600$	$R_1 = 0.0321$ $wR_2 = 0.0673$	$R_1 = 0.0319$ $wR_2 = 0.0629$	$R_1 = 0.0350$ $wR_2 = 0.0718$	$R_1 = 0.0420$ $wR_2 = 0.0686$
All data	$R_1 = 0.0485$ $wR_2 = 0.0651$	$R_1 = 0.0492$ $wR_2 = 0.0727$	$R_1 = 0.0497$ $wR_2 = 0.0680$	$R_1 = 0.0646$ $wR_2 = 0.0948$	$R_1 = 0.0836$ $wR_2 = 0.0794$
Goodness-of-fit on <i>F</i> <sup>2</sup> (all data)	10.24	1.023	1.055	1.022	0.974

Data in common: graphite-monochromated Mo K $\alpha$  radiation,  $\lambda = 0.71073$  Å;  $R_1 = \sum ||F_o| - |F_c|| / \sum |F_o|$ ,  $wR_2 = [\sum w(F_o^2 - F_c^2)^2 / \sum w(F_o^2)^2]^{1/2}$ ,  $w^{-1} = [\sigma^2(F_o^2) + (aP)^2]$ ,  $P = [\max(F_o^2, 0) + 2(F_c^2)]/3$ , where *a* is a constant adjusted by the program; goodness-of-fit =  $[\sum (F_o^2 - F_c^2)^2 / (n - p)]^{1/2}$  where *n* is the number of reflections and *p* the number of parameters.



#### 4.6. Synthesis of [ $\{\text{Co}_2(\text{CO})_6\}_2\{\mu\text{-}\eta^2\text{-}\mu\text{-}\eta^2\text{-}\text{OCH}_2\text{C}_2\text{C}_2\text{CH}_2\text{OGePh}_2\}$ ] (**6**)

To a solution of **1a** (0.50 g, 0.733 mmol) and  $\text{Cl}_2\text{GePh}_2$  (0.20 mL, 0.950 mmol) in tetrahydrofuran (150 mL) at  $-78^\circ\text{C}$ , was added *n*-BuLi (1.84 mL, 2.932 mmol). The solution was allowed to warm to room temperature and after 16 h the mixture was filtered through a florisil pad ( $2 \times 5$  cm). The solvent was removed on a rotary evaporator, the residue dissolved in dichloromethane and adsorbed onto florisil. The florisil was pumped dry and added to the top of a chromatography column. Elution with hexane afforded brown crystalline **6** (0.33 g, 50%).  $^{13}\text{C}$   $\{^1\text{H}\}$  NMR ( $\text{CDCl}_3$ ):  $\delta$  199.4 (CO), 134.4–128.6 (Ph), 101.0, 94.5 ( $\text{C}\equiv\text{C}$ ), 65.7 ( $\text{CH}_2$ ).

#### 4.7. Crystallographic studies

Single crystal X-ray diffraction data for **2**, **3**, **5a**, **5b** and **6** were collected using a Nonius-Kappa CCD diffractometer, equipped with an Oxford Cryosystems cryostream and employing Mo  $\text{K}\alpha$  ( $\lambda = 0.71073 \text{ \AA}$ ) irradiation from a sealed tube X-ray source. Cell refinement, data collection and data reduction were performed with the programs DENZO [18] and COLLECT [19] and multi-scan absorption corrections were applied to all intensity data with the program SORTAV [20]. All structures were solved and refined with the programs SHELXS97 and SHELXL97 [21], respectively. Hydrogen atoms were included in calculated positions ( $\text{C-H} = 0.96 \text{ \AA}$ ) riding on the bonded atom with isotropic displacement parameters set to  $1.5 U_{\text{eq}}(\text{C})$  for methyl H atoms and  $1.2 U_{\text{eq}}(\text{C})$  for all other H atoms. Details of the data collection, refinement and crystal data are listed in Table 6.

#### Acknowledgements

We acknowledge the financial support of the EPSRC (L.J.H.-W) and Dstl. Fort Halstead (L.J.H.-W). The help of the EPSRC mass spectrometry service, Swansea is gratefully acknowledged. Dr. John E. Davies is thanked for crystal structure determinations.

#### Appendix A. Supplementary material

CCDC 626871, 626872, 626873, 626874 and 626875 contain the supplementary crystallographic data for **2**, **3**, **5a**, **5b** and **6**. These data can be obtained free of charge via <http://www.ccdc.cam.ac.uk/conts/retrieving.html>, or from the Cambridge Crystallographic Data Centre, 12 Union Road, Cambridge CB2 1EZ, UK; fax: (+44) 1223-336-033; or e-mail: [deposit@ccdc.cam.ac.uk](mailto:deposit@ccdc.cam.ac.uk). Supplementary data associated with this article can be found, in the online version, at [doi:10.1016/j.jorganchem.2007.01.026](https://doi.org/10.1016/j.jorganchem.2007.01.026).

#### References

- [1] (a) L. Yet, *Chem. Rev.* 100 (2000) 2963; (b) M. Mori, Y. Kitamura, Y. Sato, *Synthesis* (2001) 654.
- [2] G. Illuminati, L. Mandolini, *Acc. Chem. Res.* 14 (1981) 95.
- [3] (a) I. Nakamura, Y. Yamamoto, *Chem. Rev.* 104 (2004) 2127; (b) M.E. Maier, *Angew. Chem., Int. Ed.* 39 (2000) 2073.
- [4] (a) S. Tanaka, M. Isobe, *Tetrahedron Lett.* 35 (1994) 7801; (b) C. Yenjai, M. Isobe, *Tetrahedron* 54 (1998) 2509; (c) S. Hosokawa, M. Isobe, *Tetrahedron Lett.* 39 (1998) 2609; (d) S. Hosokawa, M. Isobe, *Synlett* (1996) 351; (e) M. Isobe, S. Hosokawa, K. Kira, *Chem. Lett.* (1996) 473; (f) R. Saeeng, M. Isobe, *Tetrahedron Lett.* 40 (1999) 1911; (g) J.M. Palazon, V.S. Martin, *Tetrahedron Lett.* 36 (1995) 3549; (h) T.F. Jamison, S. Shambayati, W.E. Crowe, S.L. Schreiber, *J. Am. Chem. Soc.* 119 (1997) 4353; (i) T.F. Jamison, S. Shambayati, W.E. Crowe, S.L. Schreiber, *J. Am. Chem. Soc.* 116 (1994) 5505; (j) T. Nakamura, T. Matsui, K. Tanino, I.J. Kuwajima, *Org. Chem.* 62 (1997) 3032.
- [5] (a) A. Gelling, G.F. Mohmand, J.C. Jeffery, M.J. Went, *J. Chem. Soc., Dalton Trans.* (1993) 1857; (b) B.J. Rausch, R. Gleiter, F. Rominger, *J. Chem. Soc., Dalton Trans.* (2002) 2219; (c) A. Gelling, J.C. Jeffery, D.C. Povey, M.J. Went, *Chem. Commun.* (1991) 349; (d) F. Demirhan, A. Gelling, S. Irisli, J.C. Jeffery, S.N. Salek, O.S. Senturk, M.J. Went, *J. Chem. Soc., Dalton Trans.* (1993) 2765; (e) A. Gelling, G.F. Mohmand, J.C. Jeffery, M.J. Went, *J. Chem. Soc., Dalton Trans.* (1993) 1857; (f) F. Demirhan, S. Irisli, S.N. Salek, O.S. Senturk, M.J. Went, *J. Chem. Soc., Dalton Trans.* (1993) 453.
- [6] (a) C. Schaefer, R. Gleiter, F. Rominger, *Eur. J. Org. Chem.* (2003) 3051; (b) M.A. Brook, J. Urschey, M. Stradiotto, *Organometallics* 17 (1998) 5342; (c) R.H. Cragg, J.C. Jeffery, M.J. Went, *Chem. Commun.* (1990) 993; (d) R.H. Cragg, J.C. Jeffery, M.J. Went, *J. Chem. Soc., Dalton Trans.* (1991) 137.
- [7] (a) J.E. Davies, L.J. Hope-Weeks, M.J. Mays, P.R. Raithby, *Chem. Commun.* (2000) 1411; (b) L.J. Hope-Weeks, M.J. Mays, A.D. Woods, *J. Chem. Soc., Dalton Trans.* (2002) 1812.
- [8] V.B. Golovko, L.J. Hope-Weeks, M.J. Mays, M. McPartlin, A.M. Sloan, A.D. Woods, *New J. Chem.* 28 (2004) 527.
- [9] (a) G.F. Mohmand, K. Thiele, M.J. Went, *J. Organomet. Chem.* 471 (1994) 241; (b) A. Osella, L. Milone, C. Nervi, M. Ravera, *Eur. J. Inorg. Chem.* (1998) 1473; (c) H. Amouri, C. Da Silva, B. Malezieux, R. Andres, J. Vaissermann, M. Gruselle, *Inorg. Chem.* 39 (2000) 5053.
- [10] L.J. Hope-Weeks, M.J. Mays, G.A. Solan, *Eur. J. Inorg. Chem.*, submitted for publication.
- [11] (a) X.-N. Chen, J. Zhang, S.-L. Wu, Y.-Q. Yin, W.-L. Wang, J. Sun, *J. Chem. Soc., Dalton Trans.* (1999) 1987; (b) C.E. Housecroft, B.F.G. Johnson, M.S. Khan, J. Lewis, P.R. Raithby, M.E. Robson, D.A. Wilkinson, *Dalton* (1992) 3171.
- [12] (a) V.B. Golovko, M.J. Mays, A.D. Woods, *New J. Chem.* 26 (2002) 1706; (b) B.F.G. Johnson, J. Lewis, P.R. Raithby, D.A. Wilkinson, *J. Organomet. Chem.* 408 (1991) C9; (c) E. Champeil, S.M. Draper, *J. Chem. Soc., Dalton Trans.* (2001) 1440; (d) M.B. Nielsen, N.F. Utesch, N.N.P. Moonen, C. Boudon, J.-P. Gisselbrecht, S. Concilio, S.P. Pioletto, P. Seiler, P. Gunter, M. Gross, F. Diederich, *Chem.-Eur. J.* 8 (2002) 3601; (e) M.I. Bruce, B.W. Skelton, M.E. Smith, A.H. White, *Aust. J. Chem.* 52 (1999) 431; (f) Quan-Ling Suo, Li-Min Han, Yi-Bing Wang, Jie-Hui Ye, Ning Zhu, Xue-Bing Leng, Jie Sun, *J. Coord. Chem.* 57 (2004) 1591.
- [13] Calculated from a CCDC search, F.H. Allen, O. Kennard, *Chemical Design Automation News* 8 (1993) 31.

- [14] (a) A.J.M. Caffyn, K.M. Nicholas, in: E.W. Abel, F.G.A. Stone, G. Wilkinson (Eds.), in: L.S. Hegehus (Ed.), *Comprehensive Organometallic Chemistry II*, vol. 12, Pergamon, Oxford, 1995 (Chapter 7.1);  
(b) K.M. Nicholas, *Acc. Chem. Res.* 20 (1987) 207;  
(c) B.J. Teobald, *Tetrahedron* 58 (2002) 4133.
- [15] M. Gruselle, J.-L. Rossignol, A. Vessiers, G. Jouen, *J. Organomet. Chem.* 328 (1987) C12.
- [16] R. Guo, J.R. Green, *J. Chem. Soc., Chem. Commun.* (1999) 2503.
- [17] W.L.F. Armarego, D.D. Perrin, *Purification of Laboratory Chemicals*, 4th ed., Butterworth Heinemann, 1996.
- [18] Z. Otwinowski, W. Minor, *Methods Enzymol.* 276 (1997) 307.
- [19] R. Hooft, COLLECT, Nonius BV, Delft, The Netherlands, 1998.
- [20] R.H. Blessing, *Acta Crystallogr.* 51 (1995) 33.
- [21] G.M. Sheldrick, SHELXS97 and SHELXL97, University of Göttingen, Germany, 1997.